Cholecalciferol as Bioactive Plasticizer of High Molecular Weight Poly(D,L-Lactic Acid) Scaffolds for Bone Regeneration

TISSUE ENGINEERING: Part C
Volume 28, Number 7, 2022

DOI: 10.1089/ten.tec.2022.0041

termis
Tissue Engineering
& Regenerative Medicine
International Society

METHODS ARTICLE

Cholecalciferol as Bioactive Plasticizer of High Molecular Weight Poly(D,L-Lactic Acid) Scaffolds for Bone Regeneration

Andrea Roberto Calore, MSc,[1,2] Darya Hadavi, MSc,[3] Maarten Honing, Prof PhD,[3] Ane Albillos-Sanchez, MSc,[1] Carlos Mota, PhD,[1] Katrien Bernaerts, PhD,[2] Jules Harings, PhD,[2] and Lorenzo Moroni, Prof PhD[1]

Synthetic thermoplastic polymers are a widespread choice as material candidates for scaffolds for tissue engineering (TE), thanks to their ease of processing and tunable properties with respect to biological polymers. These features made them largely employed in melt-extrusion-based additive manufacturing, with particular application in hard-TE. In this field, high molecular weight (M_w) polymers ensuring entanglement network strength are often favorable candidates as scaffold materials because of their enhanced mechanical properties compared with lower M_w grades. However, this is accompanied by high viscosities once processed in molten conditions, which requires driving forces not always accessible technically or compatible with often chemically nonstabilized biomedical grades. When possible, this is circumvented by increasing the operating temperature, which often results in polymer chain scission and consequent degradation of properties. In addition, synthetic polymers are mostly considered bioinert compared with biological materials, and additional processing steps are often required to make them favorable for tissue regeneration. In this study, we report the plasticization of a common thermoplastic polymer with cholecalciferol, the metabolically inactive form of vitamin D3 (VD3). Plasticization of the polymer allowed us to reduce its melt viscosity, and therefore the energy requirements (mechanical [torque] and heat [temperature]) for extrusion, limiting ultimately polymer degradation. In addition, we evaluated the effect of cholecalciferol, which is more easily available than its active counterpart, on the osteogenic differentiation of human mesenchymal stromal cells (hMSCs). Results indicated that cholecalciferol supported osteogenic differentiation more than the osteogenic culture medium, suggesting that hMSCs possess the enzymatic toolbox for VD3 metabolism.

Keywords: 3D scaffolds, bone regeneration, vitamin D3, biofabrication

Impact Statement

Limitations in mechanical and biological performances of scaffolds manufactured through melt deposition may result from material thermal degradation during processing and inherent bioinertness of synthetic polymers. Current approaches involve the incorporation of chemical additives to reduce the extent of thermal degradation, which are often nonbiocompatible or may lead to uncontrolled modifications to the polymer structure. Lack of polymer bioactivity is tackled by postfunctionalization methods that often involve extra processes extending scaffold production time. Therefore, new methods to

[1]Complex Tissue Regeneration (CTR), MERLN Institute for Technology-Inspired Regenerative Medicine, Maastricht University, Maastricht, The Netherlands.
[2]Aachen-Maastricht Institute for Biobased Materials (AMIBM), Maastricht University, Geleen, The Netherlands.
[3]Imaging Mass Spectrometry Division, Maastricht Multimodal Molecular Imaging Institute (M4I), Maastricht University, Maastricht, The Netherlands.

improve scaffolds performances should consider preserving the integrity of the molecular structure and improving biological responsiveness of the material while keeping the process as straightforward as possible.

Introduction

In recent years, tissue engineering and regenerative medicine (TERM) have made huge progresses in the production of high-fidelity tissue replacements. Much of this is owing to the increasing use of well-established industrial techniques, such as additive manufacturing (AM). In fact, with respect to conventional TERM scaffold fabrication technologies, such as gas foaming/particulate leaching, freeze-drying or phase separation, AM gives full control over the morphology and high reproducibility of the manufactured scaffolds. In addition, AM technologies are compatible with both natural and synthetic polymers. Although the former provide cells with a familiar environment, the latter offer higher control and reproducibility of properties such as biodegradation and mechanical properties.[1]

One specific subclass of AM methodologies, melt-extrusion-based techniques, has emerged as one of the leading methods to fabricate scaffolds for hard tissues replacement from synthetic polymers. This success is mainly owing to the versatility of these techniques. In fact, the only requirement for the material is to be a thermoplastic and the raw material can also be provided in any form, pellets or powder, making the range of usable polymers wider than other techniques. The only limitation is for fused deposition modeling, where the feedstock must be shaped in filaments.

Other techniques, such as selective laser sintering (SLS) and three-dimensional printing (3DP), require the polymer to be in very fine powder as the resolution will depend on the granule size, whereas the material for stereolitography (SLA) must be photocurable. In addition, the needed equipment for melt-extrusion-based techniques is relatively simple as it mainly consists of a heated print head or nozzle to melt the material, and a vertically moving table. SLA and SLS require expensive lasers and additional recoating devices, whereas 3DP works with an inkjet head and a powder delivery system.[2]

For hard tissues, synthetic polymers are often the materials of reference for scaffold production. This is because of the fact that they can be designed and synthesized to cause minimal or mild foreign body reaction and can be easily modified and shaped with respect to the natural-based counterparts. Furthermore, many key properties for biological applications such as biodegradation rate, wettability, and mechanical performances can be tailored by varying their chemical structure, architecture, and molecular weight (M_w).[3,4]

An example of widely used synthetic polymers is poly (lactide) (PLA), which has found application in orthopedic implants and scaffolds for bone regeneration, thanks to its high elastic modulus (1.5–2.7 GPa).[5] High M_w grades, that is, well above the entanglement M_w, are favored because of their higher mechanical properties in the solid state.[6] However, scaffold fibers have diameters in the order of a few hundreds of micrometers and this translates into making the polymer melt flow through very narrow channels.

This results in high shear stresses, which requires driving forces like torque and temperature not always technically accessible by the equipment or imposable to chemically nonstabilized biomedical polymers, particularly of high M_w grades. This issue was highlighted by Camarero-Espinosa *et al.*,[7,8] where high M_w poly(ester)urethane had to go through a preliminary degradation step to become extrudable. Conventional ways to circumvent this issue are to reduce the material viscosity (and therefore the needed forces) with higher operating temperatures.[9]

However, some widely used polymers such as PLA, are poorly thermally stable and elevated processing temperatures might promote chain scission and M_w decrease.[10,11] Changes in the molecular structure would lead to unstable flow over processing and inhomogeneous products, which might further impact the final performances. In industry, this is often tackled by the addition of chemical stabilizers or chain extenders.

The latter have the purpose of reconnecting broken chains caused by the degradation process.[12] Commonly used compounds are tris (nonylphenyl) phosphite, polycarbodiimide, and Joncryl.[13–15] To our knowledge, there are no studies about the biocompatibility of these molecules. Tachibana *et al.*[16] found that myo-inositol, a sugar present in the human body and involved in cell signal transduction,[17] had a stabilization effect on poly(L-lactic acid) (PLLA) during processing. This was attributed to the cross-linking with esterification by the hydroxyl groups of the molecule. However, cross-linking is highly undesirable during melt-processing as it would prevent flow of the material through the extruder/printer channels.

Plasticizers represent an alternative strategy to deal with polymer degradation during processing.[18] Plasticizers are additives that have been extensively used in industry to improve the mechanical properties of inherently rigid thermoplastic polymers. They are usually low M_w molecules, which tend to separate the polymer chains and allow easier relative motion between them, increasing the matrix flexibility, softness, extensibility, and in particular their processability in terms of ease of flow.[19] Commonly used plasticizers are phthalate esters, aliphatic esters, epoxy esters, and phosphate esters.[20]

In tissue engineering (TE), citrate esters, poly(ethylene glycol), glucose monoesters, partial fatty acids, oligomeric lactic acid, and glycerol found use as plasticizers for PLA, with the goal of increasing its elongation at break and impact resistance.[21] Plasticizers appear as a more straightforward choice to improve material processability compared with chain extenders. The latter may in fact lead to unwanted and uncontrolled increase in M_w,[12] or even branching depending on the molecule active groups.[13] Such changes might negatively affect the capability of extruding the material.

Despite being potentially thermally unstable, synthetic polymers are also more bioinert compared with nonresorbable materials such as ceramics and titanium alloys, or natural polymers.[1] Biological inertness may result in poor cell activity, which in turn could lead to poor tissue development. Researchers have been trying to promote cell

responses by optimizing the scaffold material through post-treatment of the surface.[22] Techniques include plasma treatment,[23] chemical etching,[24] and chemical binding.[25] These treatments may involve some degradation of the polymer, may be nonpermanent, and may require several steps, limiting upscaling.[26]

Another strategy that has been explored is loading bioactive agents in the polymer matrix. These will be partly available on the scaffold surface and partly released over time to induce the intended effect. Yoon *et al.* fabricated scaffolds with PLGA and dexamethasone that showed anti-inflammatory effects upon the controlled release of the steroid.[27]

Bhutto *et al.* electrospun poly(L-lactide-co-caprolactone)/silk scaffolds with vitamin B5 and reported enhanced proliferation of Schwann cells cultured on scaffolds with the vitamin.[28] Damanik *et al.* blended poly(ϵ-caprolactone) (PCL) and retinoic acid, a metabolite of vitamin A1, and electrospun the mixture, which resulted in scaffolds able to enhance the synthesis of extracellular matrix proteins.[29] This type of approach has the advantages of requiring limited pre or postmanufacturing modifications, and of potentially controlling the release rate and cell response over time. However, it seems to be limited to techniques that can preserve the molecular structure, and thus the functionality, of the bioactive compound used. In fact, melt-based manufacturing would expose the additive to high temperatures, which might induce its thermal degradation and loss of bioactivity.[30]

Vitamin D is the name of a group of vitamins that play a role in the calcium and phosphate metabolism of the bone homeostasis.[31] Vitamin D3 (VD3), or cholecalciferol, is synthetized in the skin upon ultraviolet B radiation and then hydroxylated twice, first in the liver and then in the kidney, to result into the metabolically active form calcitriol.[32] Calcitriol is known to contribute not only to the differentiation of osteoblasts but also to the commitment of human mesenchymal stromal cells (hMSCs) to the osteogenic lineage.[33,34]

However, synthetic calcitriol is industrially produced through a multistep and expensive reaction making it more expensive than the precursor cholecalciferol.[35,36] Recently, it was suggested that some cell types including hMSCs, possess the enzymatic toolbox for VD3 metabolism and action, including the enzymes for cholecalciferol hydroxylation into calcitriol.[37]

In an attempt to overcome the thermal instability of PLA and its inherent biological inertness, we explored the effect of VD3 as a plasticizer. Our double goal was to reduce the processing temperature of a high-M_w amorphous PLA (poly[D,L-lactic acid] [PDLLA]) while investigating VD3 potential osteogenic effect on hMSCs.

Blends with different concentrations of VD3 were prepared by melt mixing and then characterized according to their intended use. Flow properties and thermal stability in a melt were evaluated by means of rheometry, the glass transition temperature (T_g) was measured by differential scanning calorimetry (DSC) to ensure high elastic modulus at body temperature, and mechanical properties were tested with a tensile tester. Scaffolds were then manufactured using a melt extrusion-based AM technique and cell proliferation, metabolic activity, and osteogenic differentiation were evaluated with hMSCs.

Materials and Methods

Materials

The polymer PDLLA, with an inherent viscosity midpoint of 2.0 dL/g (PDL20), was kindly provided by Corbion Biomedical (The Netherlands). VD3 was purchased from Abcam (ab143594; United Kingdom). Before any melt-based processing, the polymer was dried according to the manufacturer's protocol.

Dimethyl sulfoxide (DMSO) cell culture grade was purchased from VW and sodium hydroxide (NaOH; ≥98% [acidimetric], pellets; BioXtra) from Sigma-Aldrich. Ultra liquid chromatography (ULC)/mass spectrometry (MS)-grade water (H_2O), ULC/MS-grade methanol, liquid chromatography (LC)/MS-grade isopropanol, and LC/MS-grade dichloromethane (DCM) were obtained from Biosolve BV (Valkenswaard, The Netherlands). Ammonium acetate and cholesterol were purchased from Sigma-Aldrich.

Blending

The blend was prepared by mixing PDLLA with either 5 (PDLLA/5), 10 (PDLLA/10), or 15 (PDLLA/15) wt% VD3 in a twin-screw extruder (DSM Xplore twin-screw microextruder) preheated at 170°C, for 2 min at 150 rpm. The extrudate was cut into pellets at need.

Rheological evaluation

The complex viscosity of blends over time was measured with an Anton Paar MCR rheometer with a parallel plate geometry (25 mm diameter and 0.5 mm gap). The samples were loaded at 150°C and the time between the loading and the start of the test was kept constant between samples, at 60 s. The testing temperature was chosen to evaluate unbiased material properties as a compromise between actual processing conditions and negligible thermal degradation. The materials were subjected to a series of frequency sweeps for 120 min, from 100 to 10 rad/s at 1% strain.

The first frequency sweep per blend was used to compare the rheological behavior of the different blends. The complex viscosity versus angular frequency data were first converted to dynamic viscosity versus shear rate by means of the Cox–Merz transformation.[38] The data were then fitted with the Carreau–Yasuda model (Eq. 1):

$$\eta = (\eta_0 - \eta_\infty)\left((1 + (k\dot{\gamma})^a)^{\frac{n-1}{a}}\right) + \eta_\infty \quad (1)$$

Where η is the complex viscosity, η_0 and are, respectively, the zero-shear and infinite-shear viscosities, k the consistency (characteristic time), $\dot{\gamma}$ is the shear rate, n the power law index, and a parameter describing the transition between Newtonian plateau and power law region.[39]

The blend viscosity over time was obtained by sequentially plotting the data points at 10 rad/s for all the sweeps. The viscosity drop over time was calculated according to the following formula (Eq. 2):

$$\Delta\eta(t)[\%] = \frac{\eta(t) - \eta(0)}{\eta(0)} \times 100 \quad (2)$$

where η is the complex viscosity and t is the considered time point.

Thermal analysis

To ensure high elastic modulus of a thermoplastic polymer, it is important that the T_g is above the body temperature. This applies in particular to amorphous grades such as the PDLLA used in this study. Such class of polymers does not have a crystalline phase that could compensate for the rubbery state of the amorphous regions up to a certain extent. For this reason, the T_g of the blends was determined as midpoint through DSC with TA instruments Q2000 DSC. In brief, samples (±5 mg) in sealed in hermetic aluminum pans were heated from −20°C to 150°C at a rate of 10°C/min, cooled to −20°C, and reheated to 150°C at the same rate. Three minutes of isothermal conditions were applied at the temperature limits. Nitrogen was used as a purging gas.

Tensile testing

Dog-bone-shaped specimens for tensile testing (ISO 527-2) with 2.0 mm gauge width and 10 mm gauge length were obtained by first compression-molding 300 mg of material at 180°C for 60 s at 10 bar followed by 60 s at 240 bar. The specimens were then punched out of the film and tested at a strain rate of 100 μm/s at room temperature (RT) in a Linkam TST350 tensile stage. Elastic modulus E and yield stress σ_y were derived from the engineering stress–strain diagrams. Data are presented as average of minimum five independent replicas with error bars indicating the standard deviation.

Additive manufacturing

Scaffolds were printed using a melt extrusion-based technique (Bioscaffolder, SysENG, Germany) equipped with a G22 nozzle (DL Technology) and an in-house developed nozzle heater. After drying, the pellets from the blends or the granules of the plain PDLLA were loaded in the printhead cartridge, preheated at 190°C. The nozzle was instead preheated at 215°C in the case of PDLLA, whereas at 205°C for PDLLA/VD3. These temperatures were the result of an optimization process that led to morphologically accurate and mechanically stable scaffolds.

The liquid material was then deposited by applying a pressure of 8.6 bar and following a 0–90° pattern between layers, at a translational speed of 600 mm/min. The blends with VD3 were extruded at a screw rotation of 100 rpm, whereas for the plain PDLLA the rotation speed was set to 125 rpm. The scaffold structure consisted of blocks of $5 \times 5 \times 3\ mm^3$, with a fiber diameter of 400 μm, fiber-to-fiber (center-to-center) distance of 1 mm, and a layer thickness of 330 μm. The parameters describing the geometry of the screw and of the nozzle are given in Table 1.

Table 1. Geometric Parameters of the Screw and Nozzle Used for Scaffold Additive Manufacturing

D (mm)	*h* (mm)	*t* (mm)	*φ* (rad)	*L* (mm)	*r* (mm)	*l* (mm)
4.93	1.28	3.1	0.1975	16.6	0.2063	9.5

D is the screw outside diameter, *h* the thread depth (measured from root of screw to barrel surface), *t* the screw lead, φ the helix angle, *L* the axial length of flighted section of the screw, *r* and *l* the radius and the length of the nozzle, respectively.

Release kinetics study

Scaffold incubation. To evaluate whether any potential effect of the presence of VD3 was owing to its diffusion into the medium or to its presence on the scaffold surface, the release kinetics of VD3 from PDLLA/VD3 scaffolds were evaluated. Plain PDLLA constructs were used as reference and PDLLA/VD3 scaffolds were incubated after disinfection for 35 days in 1.5 mL of MilliQ water.

Being VD3 soluble in ethanol, scaffolds were first sterilized by treating them with oxygen plasma. In brief, they were sealed in plasma sterilization pouches, which were then placed in the chamber of a plasma cleaner (Femto PCCE) and exposed for 4 min to oxygen plasma, at a pressure of 0.53 mbar and 100 W of power.

Scaffolds were then incubated for 35 days in conditions mimicking the cell culture environment or in medium to accelerate the degradation process. In the former case, 1.5 mL of MilliQ water were used, with or without the addition of 1% DMSO (cell culture grade, BioChemica) to increase the solubility of VD3. The accelerated degradation environment consisted of 125 mM NaOH in 1.5 mL of MilliQ water, with or without the addition of 1% DMSO as well. The incubation was carried out at 37°C/5% carbon dioxide (CO_2) in sterile conditions.

At each timepoint (1, 2, 3, 7, 10, 14, 17, 21, 24, 28, 31, 35, and 37 days), the supernatant was collected and the scaffolds were placed in 1.5 mL of fresh corresponding solution. The samples were then stored at −80°C for LC-MS analysis. Samples were examined in triplicates.

Sample preparation. For LC-MS analysis the VD3 contained samples were extracted with 1.5 mL of DCM, which included 817 μM of cholesterol as an internal standard. For this extraction step, the collected samples in a 2 mL Eppendorf were transferred to 5 mL tube and the Eppendorf filled with 1.5 mL of 817 μM of cholesterol dissolved in DCM. The Eppendorf was vortex mixed for 1 min to dissolve VD3 in DCM. The content of the Eppendorf was then transferred to the same 5 mL tube and followed by vortex mixing for 1 min and 10-min centrifuge at 4000 rcf. After removing the aqueous phase of the solution, the organic phase (including DCM, cholesterol, and VD3) was kept at RT overnight to crystallize VD3 and cholesterol.

Samples were then concentrated and reconstituted with 1 mL of LC mobile phase (15–85% mobile phases A and B). Samples were ultimately transferred to 2 mL light sensitive LC vials for LC-MS analysis.

LC and MS conditions. Shimadzu LC-20AD was used for chromatic separation. Separation was achieved using Waters Corp ACQUITY UPLC CSH Fluoro-Phenyl Column, 130Å, 1.7 μm, 2.1 × 150 mm, 1/pk. The mobile phase A contained 5 mM of ammonium acetate in water and the mobile phase B contained 5 mM of ammonium acetate dissolved in methanol and isopropanol (80–20%). Chromatographic separations were performed at 40°C with the fixed flow rate of 0.18 mL/min over 9 min measurements. The

method developed as such that the starting running buffer was 85% of mobile phase B for first 3 min, which then increase to 98% over 1 min and kept at this rate until 5 min before reducing back to 85% of buffer B over 1 min.

Mass spectrometer Synapt G2Si (Waters, Milford, MA) with an electrospray ionization (ESI) source was used as a detector. The MS analysis was performed in the positive ion mode after mass calibration by sodium formate under following ESI conditions: capillary voltage of 2.5 kV, desolvation gas flow of 600 L/h, source temperature of 100°C, cone voltage of 40 V, and nebulizer gas pressure of 6.5 bar. The chromatographic data were extracted from Masslynx v4.1 (Waters) and preprocessed in Excel. The chromatograph of cholesterol was used as internal standard.

Cell seeding and culture

Cell expansion. hMSCs isolated from bone marrow were purchased from Lonza (Donor 19TL029340, male, age 24). MG-63 cells were obtained from ATCC. hMSCs and MG-63 were plated at 1000 cells/cm^2 in tissue culture flasks and cultured at 37°C/5% CO_2 in basic medium (BM), consisting of α-minimum essential medium with Glutamax and no nucleosides (Gibco) supplemented with 10 vol% fetal bovine serum (Sigma-Aldrich), until 80% confluence.

Cell seeding and culture. Scaffolds were sterilized as described in Release Kinetics Study section.

MG-63 cells were used to preliminarily evaluate any potential toxic effect of the highest concentration of VD3, for the longest acceptable period with no medium refresh, 3 days. Trypsinized cells were centrifuged at 500 rcf for 5 min and then resuspended in BM at a density of 50,000 cells/mL. About 25,000 cells/cm^2 were seeded in the wells of a 24-well plate and allowed to attach overnight. The next day (day 0), the medium was replaced with proliferation medium (PM; BM supplemented with penicillin [100 U/mL], streptomycin [100 μg/mL; Fisher-Scientific], and 200 μM L-ascorbic acid 2-phosphate [Sigma-Aldrich]) and transwells (8 μm polycarbonate pore size; Corning) with 15 wt%-loaded-VD3 scaffolds were placed on top of the wells. The culture was analyzed for metabolic activity and DNA content at day 1 and 3, with no medium refresh.

To investigate the osteogenic potential of VD3-loaded scaffolds, they were incubated overnight at 37°C/5% CO_2 in BM supplemented with penicillin (100 U/mL) and streptomycin (100 μg/mL) for protein attachment. The next day, scaffolds were placed on top of a sterile filter paper and allowed to dry. They were then placed in the wells of a non-tissue culture-treated plate.

Passage 4 hMSCs were trypsinized and centrifuged for 5 min at 500 rcf. The cells were then resuspended at a density of 150,000 cells per 37 μL in medium consisting of 10 wt% dextran (500 kDa; Pharmacosmos) in BM supplemented with penicillin (100 U/mL) and streptomycin (100 μg/mL; Fisher Scientific).[40] A 37 μL droplet of cell suspension was placed on top of each scaffold and these were incubated for 4 h at 37°C/5% CO_2 to allow cell attachment. Scaffolds were then transferred to new wells filled with 1.5 mL of PM.

The medium was replaced after 24 h and every 2 or 3 days from then on. After 7 days (day 0), scaffolds were cultured for another 35 days in PM or differentiation media (DM; PM supplemented with 10 nM dexamethasone [Sigma-Aldrich] and 10 mM β-glycerophosphate [Sigma-Aldrich]). The medium was replaced every 2 or 3 days. The culture was analyzed for metabolic activity, alkaline phosphatase (ALP), DNA content both at days 7 and 35, whereas for osteocalcin (OCN) and osteopontin (OPN) production and mineralization at day 35.

Biochemical assays

Metabolic activity. PrestoBlue™ assay (Thermo Fisher Scientific) was used to quantify cell metabolic activity. In brief, cell culture medium in sample plates was replaced with medium containing 10 v/v% PrestoBlue reagent and the sample plates were incubated in the dark at 37°C for 1 h. Fluorescence was measured at 590 nm with a plate reader (CLARIOstar®; BMG Labtech).

ALP assay. The scaffolds were washed 3× with phosphate-buffered saline (PBS) and freeze-thawed three times. Samples were then incubated for 1 h at RT in a cell lysis buffer composed of 0.1 M monopotassium phosphate, 0.1 M dipotassium phosphate, and 0.1 vol% Triton X-100, at pH 7.8. Ten microliters of cell lysate were collected and 40 μL of the chemiluminescent substrate for ALP CDP-star, ready-to-use (Roche) were added to. Luminescence (emission = 470 nm) was measured after 15-min incubation, using a spectrophotometer (CLARIOstar, BMG Labtech). Remaining cell lysates were used for DNA quantification. Values were normalized to DNA content.

DNA assay. CyQUANT Cell Proliferation Assay Kit (Thermo Fisher Scientific) was used to perform DNA assay. Samples from ALP assay were first incubated overnight at 56°C in 1 mg/mL proteinase K (Sigma-Aldrich) in Tris/ethylenediaminetetraacetic acid buffer and then freeze-thawed three more times. Subsequently, to degrade the cellular RNA, the lysate was incubated 1 h at RT in a buffer composed of 1:500 RNase A in the cell lysis buffer from the kit diluted 20× in dH_2O. The samples were then incubated for 15 min in the fluorescent dye provided by the kit (1:1) for 15 min and fluorescence was measured (emission/excitation = 520/480 nm) with a spectrophotometer. DNA concentrations were calculated from a DNA standard curve.

Enzyme-linked immunosorbent assay. The production of OCN and OPN were quantified using enzyme-linked immunosorbent assay (ELISA) kits (ab270202 and ab192143 respectively; Abcam) according to the manufacturer's instructions. In brief, at the specified time points, the supernatant from the scaffolds was collected and the protein content was quantified using the ELISA kits. The same samples were used for both assays.

Alizarin red. Calcium mineralization was quantitatively determined following a protocol from Gregory *et al.*[41]

Scaffolds were washed 3× with PBS and fixed with 4 wt% paraformaldehyde for 30 min, followed by three washing steps in MilliQ water. Subsequently, scaffolds were cut in half and each section was stained with alizarin red S (ARS) solution (60 mM, pH 4.1–4.3) for 20 min at RT. The samples were then washed with MilliQ water as long as the staining

was leaching out and then incubated for 1 h at RT with 30 vol% acetic acid while shaking. Following a 10-min incubation at 85°C, scaffolds were removed and the solutions were centrifuged at 20,000 rcf for 10 min. The pH was then adjusted to 4.1–4.3 with 5 M ammonium hydroxide and eventually absorbance was measured at 405 nm using a spectrophotometer. The concentration of ARS was calculated from an ARS standard curve and the values were normalized to DNA content.

Immunofluorescence microscopy

Samples from the osteogenic study cultured in proliferation conditions were stained with 4′,6-diamidino-2-phenylindole (DAPI) and phalloidin and imaged using immunofluorescence microscopy. In brief, samples were washed with PBS and fixed with 4 wt% paraformaldehyde for 30 min at RT, and then washed three times again with PBS. Cells were permeabilized with 0.1 vol% Triton-X for 30 min at RT, washed twice with PBS, and eventually incubated in PBS for 5 min. The whole washing sequence was repeated twice. Samples were then incubated in phalloidin solution (Alexa Fluor 568, 1:75 dilution in PBS) for 1 h at RT in the dark, under shaking. Samples were then washed three times with PBS and incubated in DAPI solution (1:300 dilution in PBS) for 15 min at RT while shaking, in the dark. Finally, samples were washed with PBS.

Confocal laser scanning microscopy was performed with a Tandem confocal system (Leica TCS SP8 STED), equipped with a white light laser (WLL). Samples were excited with the dye-specific wavelengths using the WLL or a photodiode 405 in the case of DAPI. Emission was detected with photomultiplier tubes detectors (DAPI) or hybrid detectors (phalloidin).

Statistical analysis

GraphPad Prism (version 8.4.3) was used to run statistical analysis. For the transwell study, statistical significance was assessed with a one-way analysis of variance (ANOVA) test with Tukey's *post hoc* test for comparison among the conditions in the same day. An unpaired *t*-test was used to compare the same condition between the 2 days. Statistically significant differences are marked with *($p<0.05$), **($p<0.01$), or ***($p<0.001$) when comparing the effect of different VD3 concentrations on cells at the same day and §($p<0.05$), §§($p<0.01$), or §§§($p<0.001$) when the comparing the effect of different VD3 concentrations at different time points.

The same approach was adopted to statistically evaluate the results from the osteogenic study. A one-way ANOVA test with Tukey's *post hoc* test was used for comparison among the conditions in the same culture medium. The same condition in the two different media was analyzed with an unpaired *t*-test. Statistically significant differences are marked with *($p<0.05$), **($p<0.01$), or ***($p<0.001$) when comparing the effect of different VD3 concentrations on cells at the same day and with §($p<0.05$), §§($p<0.01$), or §§§($p<0.001$) when comparing the effect of different media on cells cultured on scaffolds with the same VD3 content.

Results

Rheological evaluation

As expected, frequency sweeps showed a drop in viscosity with increasing VD3 concentration (Fig. 1A). This result is confirmed by the fitting of the Carreau–Yasuda model to the flow curves, as given in Table 2. The extrapolated data for the zero-shear viscosity η_0 showed in fact decreasing values with increasing VD3 concentration. In particular, there seemed to be a consistent drop when increasing the concentration from 5 to 10 wt%, whereas the reduction appeared to be more limited when passing from 0 to 5 and from 10 to 15 wt%.

The inverse of the parameter k gives the shear rate at which the polymer shifts from Newtonian to power-law behavior. In a log-log plot, this translates into the viscosity curve plateau at low shear rates turning into a straight line, with a transition sharpness given by a.[42] As can be seen from Table 1, increasing VD3 concentration delayed the onset of the shear-thinning region on the shear rate scale. The transition to this flow region appeared to be more or less the same for all compositions with the exception of PDLLA/15, which exhibited a smoother behavior. The slope of the power-law region is given by n, which had the same values for all the compositions.

The trend over time of the complex viscosity of the blends, and viscosity drop percentage, can be seen, respectively, in Figure 1B and C. Plain PDLLA showed an initial decrease in viscosity that reduced after 50 min, nearly reaching a plateau at $\sim$10% with respect to the viscosity value at time 0. VD3-loaded samples all exhibited an increasing trend over time, although the initial drop as well as all other data points were higher for PDLLA/15. Of note, PDLLA/5 and PDLLA/10 exhibited the lowest decrease up to 100 min of test. For longer times, their viscosity drop was higher than plain PDLLA.

Thermal analysis

The glass T_g (Table 3, extrapolated from the DSC thermograms in Supplementary Fig. S1) showed a decrease as a function of VD3 concentration, proving successful mixing and plasticization of the polymer. None of the blends showed a T_g lower than body temperature, a characteristic that would limit their use in TE applications. Besides an initial consistent decrease in glass T_g with the addition of 5 wt% of VD3, the increase of plasticizer concentration did not lead to substantial further drops in T_g.

Tensile

In Figure 1D, the stress–strain characteristic curves from tensile testing of PDLLA and PDLLA/VD3 samples are given. It immediately appears how PDLLA/10 and PDLLA/15 exhibited an unexpected lower elongation at break with respect to plain PDLLA and PDLLA/5. Data extrapolation from the curves resulted into the elastic modulus E and yield stress σ_y values as given, respectively, in Figure 1E and F.

Both elastic modulus and yield stress decreased with increasing VD3 concentration, as expected. In particular, the difference between conditions was more significant with increasing concentrations of VD3, with the drop in E and σ_y being greater for the couple PDLLA/5-PDLLA/10 than for

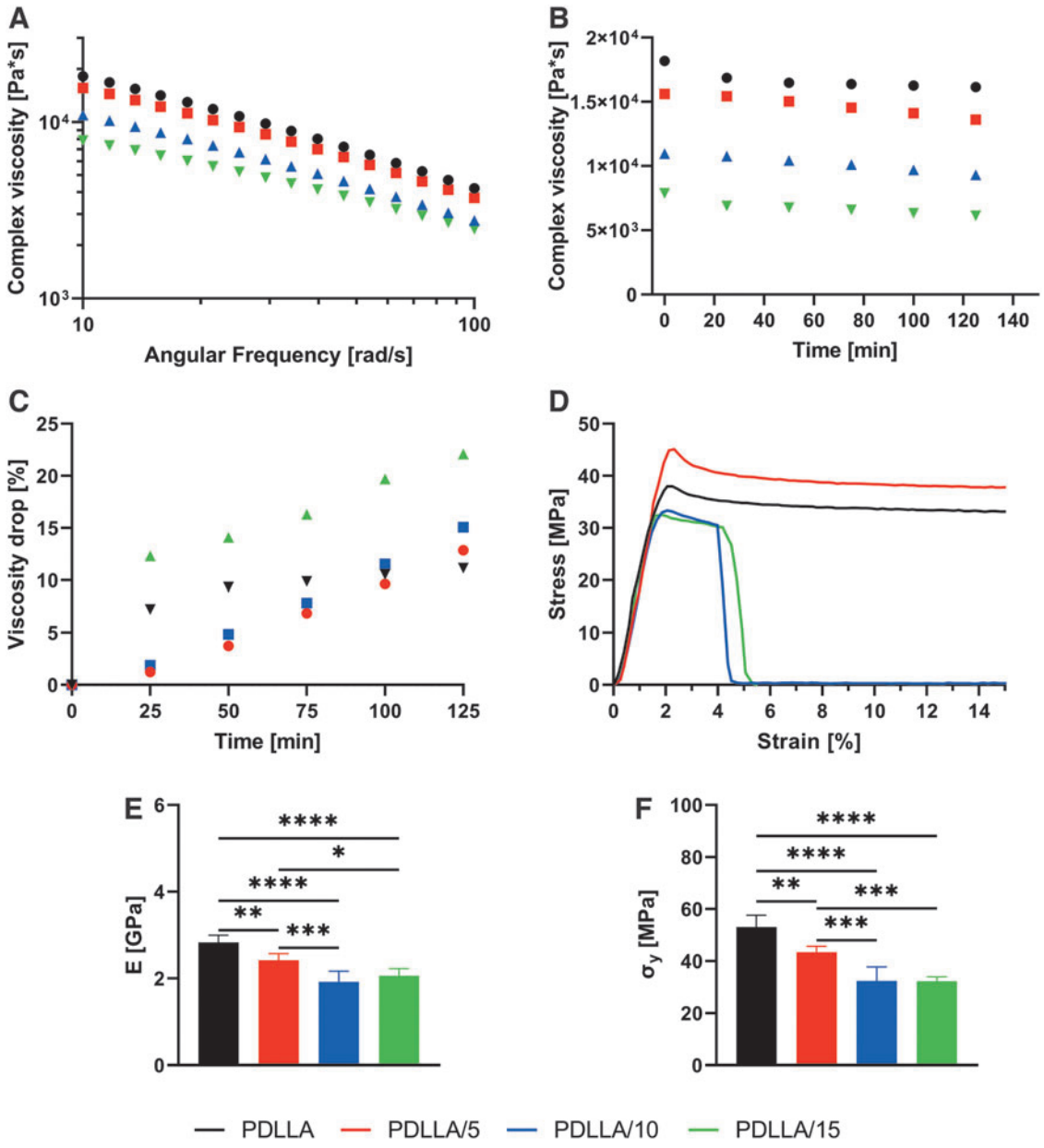

FIG. 1. **(A)** Dependence of complex viscosity on angular frequency, at 150°C. **(B)** Complex viscosity over time of plain PDLLA and PDLLA mixed with VD3 at various concentrations. Data are generated at 10 rad/s at 150°C. **(C)** Viscosity drop at the time points of **(B)** with respect to viscosity values at time 0. **(D)** Engineering stress—strain curves recorded during tensile testing. **(E)** Elastic modulus and **(F)** yield stress extrapolated from the mechanical data of PDLLA and PDLLA/VD3 samples from (**D**). Statistically significant differences are marked with *($p < 0.05$), **($p < 0.01$), ***($p < 0.001$), or ****($p < 0.0001$). PDLLA, poly(D,L-lactic acid); VD3, vitamin D3.

Table 2. Carreau–Yasuda Parameters for Poly(D,L-Lactic Acid) and Vitamin D3-loaded Poly(D,L-Lactic Acid) at 150°C

Composition	η_0 *(Pa s)*	η_∞ *(Pa s)*	k *(s)*	n	a	R^2
PDLLA	67347.96	317.96	0.11	1E-4	0.55	1
PDLLA/5	60038.14	262.14	0.10	1E-4	0.52	1
PDLLA/10	33528.95	302.95	0.09	1E-4	0.57	1
PDLLA/15	28115.33	206.33	0.04	1E-4	0.41	0.99

PDLLA, poly(D,L-lactic acid).

Table 3. Glass Transition Temperature Midpoint, Elastic Modulus, and Yield Stress of Vitamin D3 blends

Composition	T_g *midpoint (°C)*
PDLLA	57.9
PDLLA/5	50.9
PDLLA/10	50.2
PDLLA/15	49.1

T_g, transition temperature.

the couple PDLLA-PDLLA/5. Nevertheless, it can be noticed that samples PDLLA/10 and PDLLA/15 performed similarly, suggesting the existence of a saturation concentration of VD3.

Release kinetics

To study VD3 release from PDLLA, the 5, 10, and 15 wt% loaded scaffolds were submerged in four different types of media consisting of distilled water, distilled water with 1% DMSO, distilled water with 125 mM NaOH, distilled water with 125 mM NaOH, and 1% DMSO.

The LC-MS analysis on the collected samples from the medium with pure distilled water and distilled water with 1% of DMSO showed no chromatographic peaks pertaining to VD3. This observation implies the absence of VD3 in the collected samples from day 1 until day 37.

However, the collected samples from NaOH containing media (with and without DMSO) showed chromatographic peaks relating to oxidized form of VD3 at mass over charge ratio (m/z) of 383 Dalton. The average amounts of VD3 and their relative standard deviation per time interval are given in Table 4, for samples incubated in NaOH, and Table 5, for samples incubated in NaOH + DMSO. Plotted VD3 release profiles showed an irregular release pattern of VD3 in the absence of DMSO (Fig. 2A), especially at lowest concentrations of VD3.

Instead, the release profile in the presence of DMSO exhibited a more sustained trend (Fig. 2B). On the contrary, the collected samples from only NaOH containing medium (Table 4) exhibited higher total amount of VD3 than NaOH + DMSO medium (Table 5) for all concentrations of scaffold except for the 10 wt% D3 loaded. In addition, a burst release was observed between days 3 and 7 in all scaffolds on both types of medium, except for 10 wt% VD3-loaded scaffold in NaOH medium.

Table 4. Release Kinetics Data from Poly(d,l-Lactic Acid)/Vitamin D3 Scaffolds Incubated in Sodium Hydroxide

	PDLLA/5		*PDLLA/10*		*PDLLA/15*	
Day	*APAC*	*RSD (%)*	*APAC*	*RSD (%)*	*APAC*	*RSD (%)*
1	0.78	9.6	0.02	26.0	0.04	126.1
2	0.34	53.4	0.02	17.9	0.01	129.9
3	0.09	106.2	0.03	47.8	0.01	144.3
7	0.95	44.5	0.05	53.8	0.83	135.9
10	2.17	62.1	0.16	101.3	1.21	138.3
14	0.60	24.5	0.40	65.5	2.24	84.6
17	0.19	122.4	0.61	87.6	3.35	86.8
21	0.24	40.1	1.23	77.3	10.32	102.1
24	0.60	65.2	2.61	67.9	12.92	118.2
28	1.11	76.4	2.98	39.1	4.97	43.6
31	1.55	77.5	5.16	62.5	3.98	23.6
35	1.33	110.8	3.87	32.2	5.10	55.3
37	7.63	86.3	4.26	13.7	3.23	11.9
Total	17.14		21.41		48.21	

Data are expressed as APACs with their RSD (%) and total release amount.

APAC, average peak area counts; RSD, relative standard deviation.

Table 5. Release Kinetics Data from Poly(d,l-Lactic Acid)/Vitamin D3 Scaffolds Incubated in Sodium Hydroxide + Dimethyl Sulfoxide

	PDLLA/5		*PDLLA/10*		*PDLLA/15*	
Day	*APAC*	*RSD (%)*	*APAC*	*RSD (%)*	*APAC*	*RSD (%)*
1	0.28	12.5	0.01	15.8	0.00	35.6
2	0.59	31.7	0.11	29.2	0.00	63.2
3	0.14	75.3	0.07	9.8	0.00	48.3
7	1.31	99.2	0.64	90.5	1.34	56.1
10	2.24	104.2	0.90	70.7	1.90	65.7
14	1.13	72.5	1.44	18.8	1.26	20.3
17	0.48	32.5	1.49	76.4	0.94	6.8
21	0.78	65.2	2.84	57.2	1.19	39.4
24	0.31	14.8	2.79	55.0	0.78	42.1
28	1.30	72.8	4.80	9.0	1.46	68.4
31	1.50	37.6	4.83	46.5	1.22	24.1
35	1.32	69.3	4.42	19.7	1.16	28.7
37	1.78	75.7	5.43	0.8	0.53	41.9
Total	12.64		29.76		11.79	

Data are expressed as APACs with their RSD (%) and total release amount.

Cell studies

Biocompatibility. To evaluate any potential cytotoxic effect by the VD3 concentrations used, a biocompatibility study was run over 3 days. At day 1, all the samples showed comparable DNA amounts (Fig. 3A). The same result was seen at day 3 as well. Over the 3 days of culture, only PDLLA/15 samples showed a statistically relevant increase in DNA between days 1 and 3.

In terms of metabolic activity, all conditions resulted in comparable value, both at days 1 and 3 (Fig. 3B). Between days 1 and 3, metabolic activity increased significantly only for cells cultured on PDLLA/5 scaffolds.

Osteogenicity. The different concentrations of VD3 in the additive-manufactured scaffolds were tested for osteogenic effects on hMSCs. Cells were cultured on plain PDLLA scaffolds and on constructs loaded with 5, 10, and 15 wt% VD3. The culture lasted up to 35 days, in proliferation or mineralization conditions, after 7 days of proliferation.

At both time points, cells displayed comparable metabolic activities among scaffolds and media. At day 7 (Fig. 4A), cells seemed to have proliferated homogeneously on all scaffolds in PM, except for those cultured on PDLLA/10. Cells cultured in mineralization conditions displayed instead lower proliferation, with particular reference to cultures on PDLLA/10 and 15 scaffolds. At the second time point (Fig. 4C), the differences were less pronounced, with cells in basic conditions being in comparable amount with those cultured in DM. Of note is that PDLLA scaffolds showed higher DNA content than VD3-loaded scaffolds.

From Figure 4B and D, it can be seen that the addition of VD3 in the scaffolds did not have any impact on cell metabolic activity. In fact, cells cultured on VD3-loaded scaffolds showed a metabolic activity comparable with those grown on plain PDLLA constructs at both time points, day 7

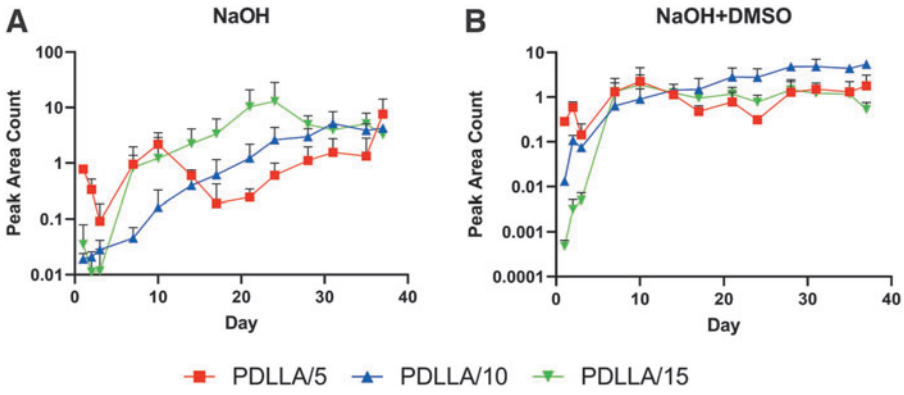

FIG. 2. Release profile of VD3 from PDLLA/VD3 scaffolds incubated in **(A)** NaOH medium and **(B)** NaOH + DMSO medium. The release profile is expressed as peak area count per single time point. DMSO, dimethyl sulfoxide; NaOH, sodium hydroxide.

(Fig. 4B) and day 35 (Fig. 4D). In addition, cells in each condition maintained a steady metabolic activity over the culture period, as shown by the comparable results.

In basic conditions, ALP, OPN, and OCN generally showed upregulated values for scaffolds with 10 and 15 wt% VD3, at both time points (Fig. 5A–F). At day 7, cells cultured on PDLLA/10 and 15 showed enhanced ALP production compared with those on other scaffold types, whereas at day 35 PDLLA/15 exhibited the highest secretion. OPN showed a substantially stable profile over time, whereas OCN seemed to increase, with cells cultured on PDLLA/10 and on PDLLA/15 scaffolds exhibiting the highest production.

Markers secretion in mineralization conditions followed a similar trend (Fig. 5A–F). ALP secretion (Fig. 5A, B) resulted in an increase over time, with cells on PDLLA/5 and PDLLA/10 scaffolds showing higher activity than other conditions at day 35. OPN secretion (Fig. 5C, D) did not significantly change although, at day 7, it exhibited the same profile as in PM, with PDLLA/10 scaffolds slightly standing out. Instead, a decrease in OCN (Fig. 5E, F) production could be noticed over time. Once again, the profile at day 7 followed the one in basic conditions. Overall, there seemed to be limited differences between the two media conditions, except for OCN secretion at day 35. Here, cells cultured on VD3-loaded scaffolds showed enhanced production of OCN in basic conditions with respect to MM.

ARS staining and its quantification (Fig. 5G) showed significantly higher calcium deposition for the compositions PDLLA/10 and 15 in basic conditions. In MM instead, all three VD3 compositions exhibited higher amounts of calcium than the control PDLLA scaffold, although with substantial variation among the samples.

Immunofluorescence microscopy

VD3 is a relatively hydrophobic compound that might influence the protein adsorption pattern on scaffolds surface and, consequently, cell morphology. As it is known that stem cell morphology can influence cell differentiation, we investigated cell adhesion and spreading by confocal microscopy (Fig. 6 and Supplementary Fig. S2). Cells in MM conditions at 7 days showed a relatively regular cell pattern on all scaffold types, with cells majorly aligned along the scaffold fiber (Supplementary Fig. S2). Cell cultured on PDLLA and PDLLA/5 exhibited a degree of transversal orientation. Immunofluorescence images at day 7 in PM showed similar cell morphology (data not shown).

We further investigated changes in cell morphology at day 35. Cells cultured for 35 days in PM appeared to have reached confluence and covered the scaffold filaments surface (Fig. 6). No major differences in morphology could be seen, with most of the cells exhibiting an elongated shape along the fiber axis. Some cells cultured on PDLLA/10 scaffolds seemed to have aligned transversally with respect to the scaffold filament. Cells cultured for 35 days in MM exhibited a morphology similar to those grown in PM (data not shown).

Discussion

PLA is a well-known polymer widely used in hard TE because of its biocompatibility and excellent mechanical properties.[1] However, it exhibits unstable properties when processed in a liquid state at high temperatures, which hinders its use as scaffold material with melt-based AM techniques. Tachibana *et al.*[16] noticed that the blending with

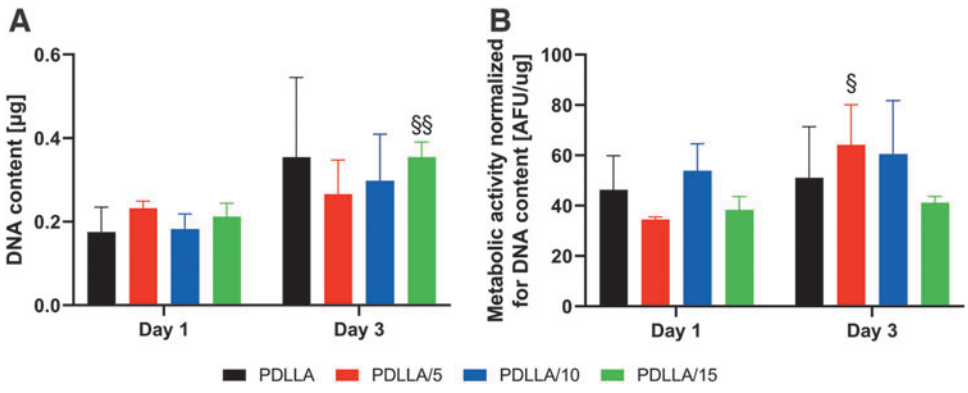

FIG. 3. **(A)** DNA content and **(B)** metabolic activity from the biocompatibility study. Symbols §($p < 0.05$) or §§($p < 0.01$) indicate statistically significant differences when comparing the effect of different VD3 concentrations at different time points.

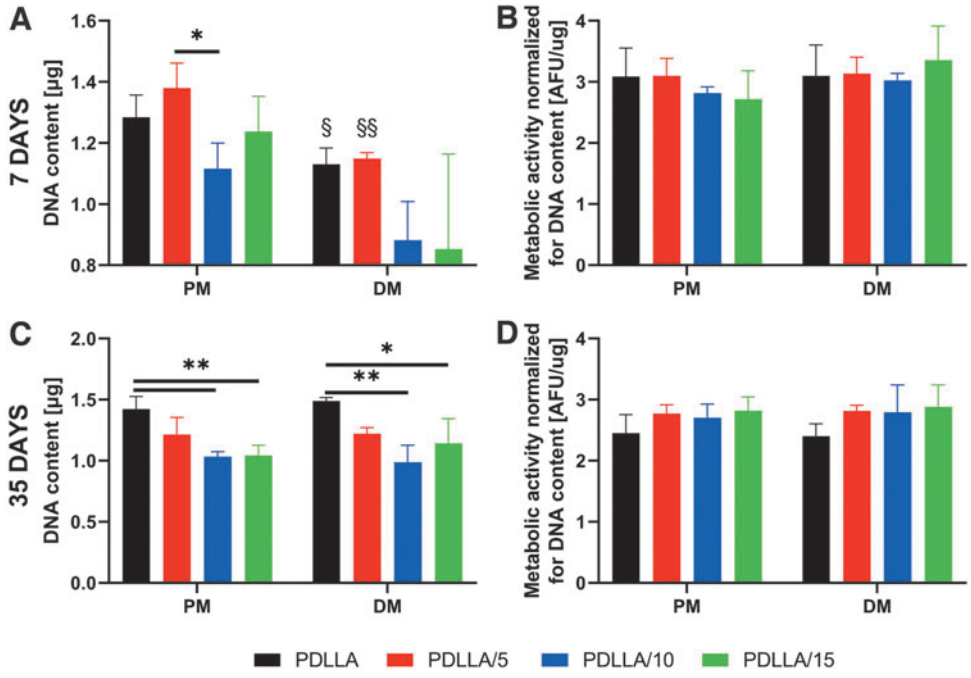

FIG. 4. DNA content and metabolic activity from the osteogenic study, after 7 **(A, B)** and 35 **(C, D)** days. Statistically significant differences are marked with *($p<0.05$) or **($p<0.01$) when comparing the effect of different VD3 concentrations on cells at the same day and with §($p<0.05$) or §§($p<0.01$) when comparing the effect of different media on cells cultured on scaffolds with the same VD3 content.

myo-inositol limited the drop in M_w during processing. They attributed this result to chain extension. Kang *et al.*[43] blended PLLA with PCL and magnesium hydroxide to improve, respectively, its brittle behavior and neutralize the acidic moieties from thermal degradation. They indeed observed that the addition of magnesium hydroxide alleviated the M_w reduction by inactivating the chain end groups and degrading byproducts capable of backbiting reactions and hydrolysis.

Nevertheless, these approaches do not solve the issue of processing high M_w grades if not by increasing the operating temperature, which in turn would accelerate the degradation rate.[44]

As highlighted by Camarero-Espinosa *et al.*,[7,8] an initial degradation step is sometimes necessary to enable extrusion of high M_w thermoplastic polymer grades using the Bioscaffolder technology. In their study, a poly(ester)urethane had to be thermally degraded to enable its extrusion through the printer nozzle. In particular, the polymer M_w was reduced from 125,771 to 80,295 kg/mol by keeping the material isothermally in the printer reservoir for 1 h. Such strategy is sometimes needed because the torque necessary to provide a certain flow rate in an extruder, or in a screw-driven printer such as the one used by Camarero-Espinosa *et al.* and us, is directly proportional to the zero-shear viscosity of the polymer melt.[45] This is in turn proportional to M_w according to the formula $\eta_0 \sim M_w^{3.4}$.[39]

Therefore, polymer grades of higher M_w require higher torque applied to the screw at a constant temperature. In our study, we evaluated the performances of a plasticizer to reduce the viscosity (and therefore the mechanical and thermal energy requirement for extrusion) of a high M_w PDLLA. To not limit the scope of the plasticizer to the manufacturing process, we chose a molecule with known physiological roles such as cholecalciferol, to investigate its additional bioactive potential on hMSCs.

The rheological results confirmed that the plasticization occurred effectively. This is evident from the decreasing trend of zero-shear viscosity with VD3 concentration: the higher the amount of plasticizer, the lower resistance to flow. The effect of plasticization on k, which is a material relaxation time, is also noteworthy: with higher amounts of VD3, the polymer macromolecules take shorter to relax after the cessation of a stress, causing them to be more mobile. In fact, when low M_w plasticizers dissolve properly in the polymer matrix, they diffuse between the macromolecules generating free volume and ease of movement, just as an increase in temperature would.[6] This will result in deformation occurring at lower stress and strain values,[46] which implies lower energy to induce material flow during processing.[47]

Of interest, the concentration of plasticizer did not seem to have an effect on the slope in the shear-thinning region. This part of the flow curve describes orientation and stretching of the polymer chains along the direction of shear: at low shear rates (smaller than the reciprocal Rouse relaxation time) orientation dominates and is accompanied by disentanglement of the molecules while stretching becomes more and more significant at increasing shear rates.[48,49]

The identical values for n suggest that the plasticizer had no influence at the shear rates corresponding to the power-law region, where the polymer molecules were already sufficiently disentangled to render the plasticizer unnecessary. Instead, at those lower shear rates corresponding to the Newtonian plateau and the transition region, the chains were still in an entangled state, and the presence of the plasticizer played an effective role in determining a difference in the rheological curve for different concentrations.

The results from the time sweeps showed that the presence of VD3 did not have any appreciable stabilization effect. Whereas the drop in viscosity of PDLLA stabilized after an initial decrease, samples containing VD3 showed a reduction in viscosity increasing over time. This trend suggests that VD3 might be degrading for long residence times at such temperatures, as suggested by Pelc and Marshall[50] and Jakobsen and Knuthsen.[51] Thermal degradation results

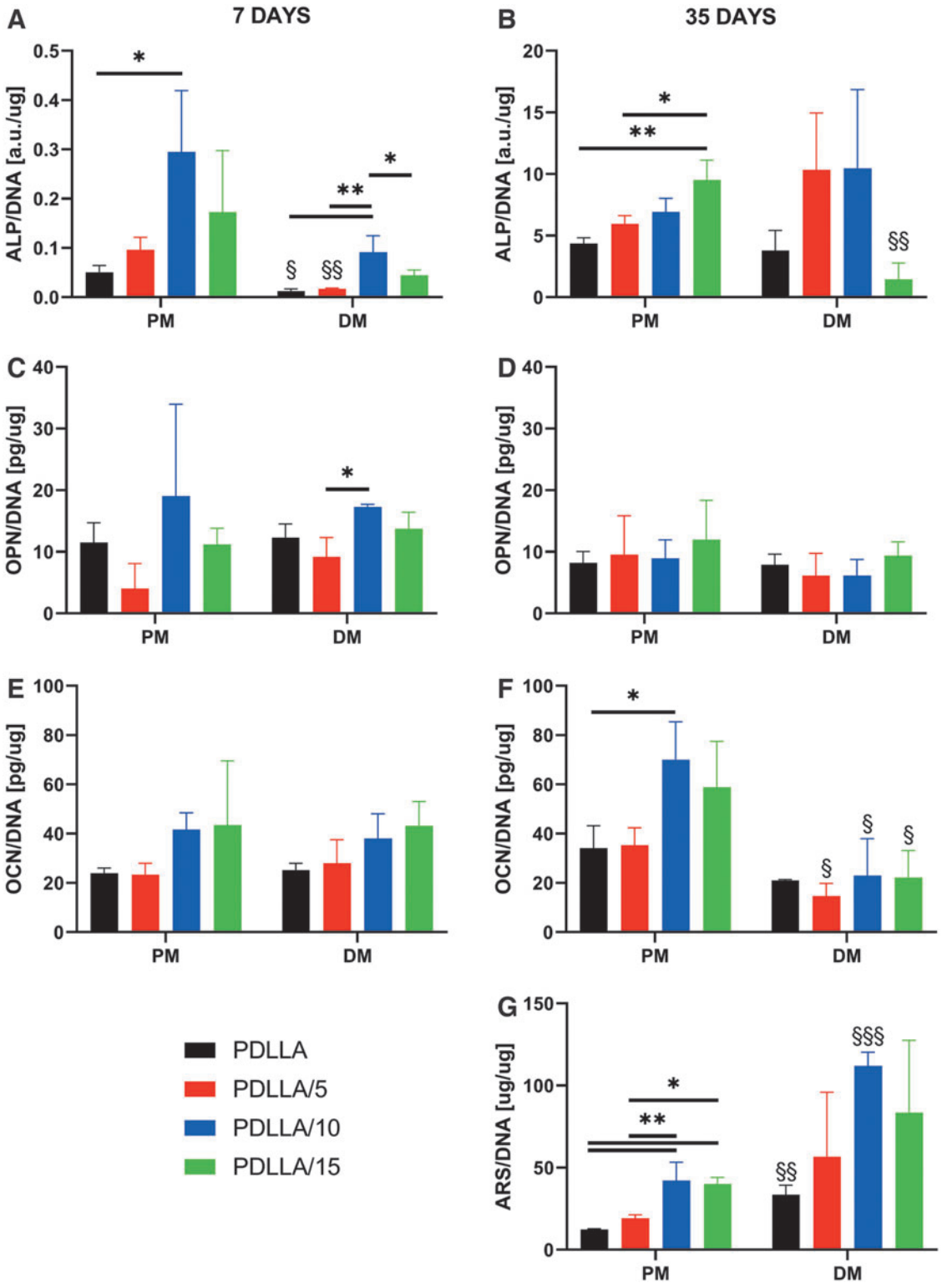

FIG. 5. ALP **(A, B)**, OPN **(C, D),** and OCN **(E, F)** secretion from the osteogenic study at day 7 (*left column*) and at day 35 (*right column*). Results from day 35 include the quantification of calcium deposition via Alizarin red staining **(G)**. Statistically significant differences are marked with *($p<0.05$) or **($p<0.01$) when comparing the effect of different VD3 concentrations on cells at the same day and with §($p<0.05$), §§($p<0.01$), or §§§($p<0.001$) when comparing the effect of different media on cells cultured on scaffolds with the same VD3 content. ALP, alkaline phosphatase; OCN, osteocalcin; OPN, osteopontin.

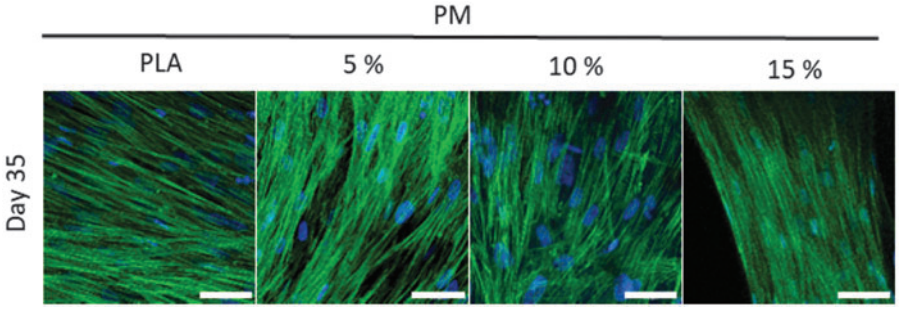

FIG. 6. Immunofluorescence images of cells cultured for 35 days on all the scaffold types, in proliferating conditions, from the osteogenic study. Cell nuclei stained with DAPI are given in *blue*, whereas actin filaments stained with phalloidin are given in *green*. The scale bar represents a distance of 50 μm.

in compounds of lower M_w, which are responsible for the decrease in viscosity as explained previously. However, it is important to note that all blends were tested at the same temperature. Instead, the addition of VD3 allows the processing to be carried out at lower temperatures thanks to its plasticization effect, being the zero-shear viscosity (and therefore the torque requirement for extrusion) lower.

Carley and Strub[52] derived the expression for the power required to drag a Newtonian polymer melt through the screw channel against the back pressure originated by the presence of the nozzle, which is given in (Eq. 3):

$$Z = \eta N^2 \left(\omega + \frac{\alpha\gamma}{\beta + k}\right) \tag{3}$$

where η is the zero-shear rate viscosity of the polymer melt, N is the screw rotating speed in revolutions per second (RPS) and ω, α, γ, β, and k are parameters containing only the dimensions of the screw and the nozzle and defined as follows:

$$\omega = \frac{\pi^3 D^3 L}{h} \tag{4}$$

$$\alpha = \frac{\pi D h t \cos^2\phi}{2} \tag{5}$$

$$\gamma = \frac{\pi^2 D^2 h \tan\phi}{2} \tag{6}$$

$$\beta = \frac{h^3 t \sin\phi \cos\phi}{12L} \tag{7}$$

$$k = \frac{\pi r^4}{8l} \tag{8}$$

Here, D, h, t, φ, L, r, and l are as described in Table 1. By dividing the power Z (Eq. 3) by the screw rotation speed N, the torque T is obtained[45]:

$$T = \frac{Z}{N} \tag{9}$$

In the lab-scale printer used in this study, the torque provided by the stepper motor to the screw is abundantly lower than in the case of similar industrial printers and extruders, being the required throughput also reduced. For this reason, the processing temperatures have to be higher so as to favor the flow of the polymer melt through the screw channel and the nozzle. The low flow rate coupled to the high processing temperatures allows to make the assumption of Newtonian behavior of the polymer melt during deposition. Therefore, taking η as the zero-shear rate values of Table 2, Equation 9 allows the calculation of the torque required to extrude the grades used in this study at given screw RPS.

The extrusion of PDLLA/5 requires 10% less torque than that of PDLLA, the extrusion of PDLLA/10 is 50 and 44% less demanding than PDLLA and PDLLA/5, respectively, and depositing PDLLA/10 requires 42%, 47%, and 84% of the torque needed for PDLLA, PDLLA/5, and PDLLA/10, respectively. For this reason, the extrusion temperature of each grade could be lowered according to the torque requirement, thus slowing the degradation process, which is directly correlated to temperature itself.[44]

In addition, plasticization is also accompanied by a decrease in the T_g of the polymer.[46,53,54] For this reason, we verified whether this occurred to the extent of dropping below body temperature. Because PDLLA is amorphous, a T_g lower than 37°C would result in rubbery and deformable implants. The results showed that the glass T_g did not excessively drop, allowing the safe use of this blend for TE purposes.

Polymer plasticizers have generally the objective of increasing flexibility and toughness of the matrix while often contributing to a reduction in strength.[21] This is achieved by separating the polymer chains and thus allowing easier relative motion.[19] The addition of VD3 to PDLLA, a noteworthy stiff and brittle material with low deformation at break,[5,55] effectively reduced its modulus, although to a limited extent.

Nevertheless, we noticed that compositions with the highest plasticizer content unexpectedly exhibited lower elongation at break. Martin and Averous[21] suggested that such behavior could originate from lack of affinity between the materials, although the mechanical properties alone could not be considered absolute evidence of noncompatibility and consequent phase separation. Rheological and DSC data seemed to confirm the miscibility of the two materials to molecular levels.

However, these tests were conducted at temperatures that allow mobility in the system. We hypothesize that, upon cooling, some segregation might have taken place, the extent of which might have been higher for higher VD3 concentrations. In addition, excessive amount of such a low M_w plasticizers might have reduced the entanglement network strength, with detrimental effects on the mechanical properties. These two phenomena could have been responsible for the unexpected mechanical data for PDLLA/10 and PDLLA/15, the blends with indeed the highest VD3 content.

The absence of VD3 in the collected samples from distilled water media (with and without DMSO) could be owing to the poor solubility of VD3 as well as PDLLA in

water. The insolubility property could result in the aggregation of both molecules on the surface of the scaffold rather than diffusion into the medium. However, the addition of NaOH to the media could enhance the surface hydrophilicity of PDLLA by imposing alkaline hydrolysis and speeding up polymer degradation, as explained previously.[56] The higher release amount of VD3 in NaOH medium in contrast to NaOH + DMSO containing medium could indicate the detrimental effect of DMSO on release profile.

In the presence of DMSO, the miscibility of VD3 in PDLLA increases, which in turn reduced the diffusion rate of this plasticizer from polymer into the media. Similar finding has been reported for the release of doxorubicin from PLA polymer in the presence of DMSO.[57] In addition, the polar aprotic nature of DMSO that dissolves both polar and nonpolar compounds could have enabled sustained release of VD3. However, VD3 is only sparingly soluble in DMSO,[58] which could explain the lower total amount of this plasticizer in NaOH + DMSO than only NaOH-containing medium. On the contrary, in the absence of DMSO, the release of VD3 was mainly dependent on polymer degradation, which was accelerated by NaOH. Furthermore, the irregular release pattern in NaOH medium could imply the inhomogeneous blend of VD3 in PDLLA.

As explained by Utracki and Wilkie,[55] low M_w compounds in a polymer matrix tend to migrate toward the region with the highest shear rate, thus lowering the energy state of the system. In the case of capillary flow such as the flow in the printer nozzle, the highest shear rate is located at the capillary walls. This should have led to an evenly distributed concentration of VD3 on the scaffolds surface, given a sufficiently long nozzle for full flow development. However, in the equipment used for this study, the fluid flowing through the nozzle arrives from a screw channel, where the flow profile is rather different.[45,59] In particular, the shear rate is not axisymmetric but develops linearly from a null value at the barrel wall to its maximum at the screw root.

We hypothesize that the length/diameter ratio of the nozzle in use was not sufficiently high for the flow to fully develop from the profile in the screw channel to that of a proper capillary. This could have resulted in an inhomogeneous distribution of VD3 over the filament cross-section. In addition, although by increasing the loading percentage of VD3 the overall release amount of this molecule raised in both media, this relation was not true for 10 wt%-loaded scaffolds. This observation emphasizes on the importance of release behavior rather than the loading percentage of VD3 in PDLLA for drug delivery applications.

VD3 or cholecalciferol is known to be involved in bone metabolism[33,34,37] but to our knowledge there are not many examples of its use for TE purposes.[60,61] In this study, relatively high concentrations were used, which could have had toxic effects on cells. For this purpose, a transwell study was conducted. Results showed comparable proliferation and metabolism for cells cultured on plain and VD3-loaded scaffolds, meaning that the plasticizer did not induced any cytotoxicity.

On the contrary, PDLLA/15 scaffolds showed greater proliferation with respect to the other groups, which remains unexplained as several authors reported the antiproliferative properties of VD3.[31,33,62,63] In addition, cells cultured on PDLLA/5 scaffolds exhibited an increase in metabolic activity over the culture. As highlighted by Calore *et al.*,[64] the PrestoBlue assay used here is based on the reduction of resazurin to resorufin by mitochondrial activity, which is often increased during differentiation.

During the osteogenic study, cells showed to be similarly metabolically active on all scaffold types and in both media, indication that the high concentration of VD3 did not have any toxic effect on cultures longer than 3 days. The proliferation data showed lower cell amount for scaffolds with 10 and 15 wt% VD3, which we hypothesize is owing to the probable higher concentration of the plasticizer on the fibers surface. VD3 is, in fact, relatively hydrophobic[65] and this characteristic might have affected the initial amount of attached cells. Comparing data from day 7 with 35, it seems that cells cultured on VD3-loaded scaffolds did not proliferate. This appears to be in line with previous studies,[34,62,66] where the antiproliferative effect of VD3 was reported.

The trend shown by the osteogenic markers in basic conditions suggests that cells cultured on PDLLA/10 and 15 scaffolds might be in the mature osteoblast phase, when mineralization is still in an early phase. This is suggested in particular by the significantly higher amount of deposited calcium and the peaks in OCN amounts, whose secretion is known to be VD3 responsive.[67] According to Aubin,[68] during osteogenic differentiation ALP increases until mineralization is well progressed, at the beginning of which OCN appears.

PDLLA/10 and 15 conditions showed increasing ALP and OCN over the culture, in addition to greater calcium deposition compared with the other scaffolds. This could not be further supported by immunofluorescence images, where cells showed comparable morphology over all culture conditions and no specific lineage-related change could be noted. OPN is supposed to peak twice during proliferation and once more before the upregulation of OCN.[68]

In this study, we did not see any condition inducing enhanced OPN secretion. We suggest that the chosen time points did not temporally match the OPN peaks. Nevertheless, we expect that the peaks relative to proliferation would have pertained only to the PDLLA scaffolds, whereas PDLLA/10 and 15 would have shown that peak supposed to appear right before OCN. It is important to note how cells cultured on PDLLA/5 exhibited the same behavior of those grown on PDLLA. This suggests that there might be a threshold concentration below which there seem to be no osteogenic effect on cells. Such a possibility arises from the potential inhomogeneous distribution of VD3 over the filament cross-section as previously explained, which would not only influence both the plasticizer availability per unit of time but also the release profile over the whole culture period.

In mineralization conditions, cells cultured on VD3-loaded scaffolds did not generally show significant differences in osteogenic markers secretion compared with cells grown on plain PDLLA. Despite the wide variations, ARS data suggest that VD3 enhanced mineralization. ALP values seem to support this finding for PDLLA/5 and 10 scaffolds, suggesting the presence in the mature osteoblast phase. It is important to note that Aubin[68] suggested that the secretion of bone lineage proteins is often heterogeneous in individual cells but mainly mineralization is the clearest expression of osteogenic differentiation. The low ALP values for PDLLA/

15, coupled with the presence of deposited calcium, might be the sign of an even more advanced differentiation stage, for which it would be then plausible to observe a lower OCN secretion.

Comparing the cell behavior in the two different environments shows that the coupled presence of VD3 and dexamethasone might have a lower impact on osteogenesis than the sole VD3.

Overall, the results seem to suggest that the metabolically inactive cholecalciferol can promote osteogenic differentiation *in vitro* as well as its active metabolite calcitriol. This supports the finding that hMSCs have the enzymatic toolbox to metabolize VD3 into the active form calcitriol.[37] Current *in vitro* osteogenic protocols include the use of dexamethasone, a steroid that is not present *in vivo* or regulates the physiological differentiation of osteoblast precursors.[69] Costa *et al.*[70] pointed out that dexamethasone has toxic effects at concentrations above 1000 nM and that severe bone loss and osteoporosis were associated with prolonged treatments with dexamethasone. Our study suggests that cholecalciferol could not only be considered a cheaper alternative to calcitriol but also a less harmful substitute of dexamethasone for TE purposes.

Nevertheless, our results derive from the specific processing conditions used. In fact, Wubneh *et al.*[71] suggested that drug concentration and spatial distribution are controlled by the fabrication process, and highly impact the drug effectiveness and release rate. As a blend morphology is a complex interplay between material properties and processing conditions,[55] future studies should aim at evaluating the effect of different manufacturing parameters (namely, shear rate) on the distribution of VD3 within the scaffold fiber, and the resulting release kinetics and osteogenic potential.

Conclusions

This study presents the plasticization of a commonly used synthetic polymer to decrease its melt viscosity, and therefore the energy requirements for extrusion, with potential reduction of thermal degradation. In addition, the adoption of such strategy allows the processing of those high M_w grades that might require an initial degradation step for extrusion. The materials were blended in melt state to evaluate the feasibility of mixing directly in the printer, to obtain a single-step process. Rheological evaluation confirmed a reduction in viscosity, whereas DSC measurements and tensile testing revealed a pronounced drop in glass transition and mechanical properties with the addition of VD3.

However, the drop in performance is reduced for higher concentrations of the plasticizer. This will not hinder performances in a biological environment. Furthermore, we report that the plasticizer of choice, the metabolically inactive cholecalciferol, seemed to support osteogenic differentiation and mineralization as much as mineralization culture conditions, confirming the presence in hMSCs of the enzymatic toolbox for VD3 metabolism.

Acknowledgment

Some of the materials were kindly provided by Corbion Purac Biomaterials (The Netherlands).

Disclosure Statement

No competing financial interests exist.

Funding Information

This work was financed by Brightlands Material Center and by the Dutch Province of Limburg.

Supplementary Material

Supplementary Figure S1
Supplementary Figure S2

References

1. Van Blitterswijk, C.A., and De Boer, J., eds. Tissue Engineering: Second Edition [Internet]. Cambridge, United States: Elsevier, 2014. Available from: https://linkinghub.elsevier.com/retrieve/pii/B9780124201453000146
2. Mota, C., Puppi, D., Chiellini, F., and Chiellini, E. Additive manufacturing techniques for the production of tissue engineering constructs. J Tissue Eng Regen Med **9,** 174, 2015.
3. Middleton, J.C., and Tipton, A.J. Synthetic biodegradable polymers as orthopedic devices. Biomaterials **21,** 2335, 2000.
4. Hutmacher, D.W. Scaffold design and fabrication technologies for engineering tissues—State of the art and future perspectives. J Biomater Sci Polym Ed **12,** 107, 2001.
5. Hoying, J.B., and Williams, S.K. Essentials of 3D Biofabrication and Translation. In: Atala, A., and Yoo, J.J., eds. Winston-Salem, NC: Elsevier, 2015. Available from: http://www.sciencedirect.com/science/article/pii/B9780128009727000190
6. Osswald, T., and Rudolph, N. Polymer Rheology [Internet]. München: Carl Hanser Verlag GmbH & Co. KG, 2014. Available from: http://www.hanser-elibrary.com/doi/book/10.3139/9781569905234
7. Camarero-Espinosa, S., Calore, A.R., Wilbers, A., Harings, J., and Moroni, L. Additive manufacturing of an elastic poly(ester)urethane for cartilage tissue engineering. Acta Biomater **102,** 192, 2020.
8. Camarero-Espinosa, S., Tomasina, C., Calore, A.R., and Moroni, L. Additive manufactured, highly resilient, elastic, and biodegradable poly(ester)urethane scaffolds with chondroinductive properties for cartilage tissue engineering. Mater Today Bio **6,** 100051, 2020.
9. Calore, A.R., Sinha, R., Harings, J., Bernaerts, K.V, Mota, C., and Moroni, L. Chapter 7: Thermoplastics for tissue engineering. In: Rainer, A., and Moroni, L., eds. Computer Tissue Engineering, 2021, pp. 75–99.
10. Ragaert, K., Dekeyser, A., Cardon, L., and Degrieck, J. Quantification of thermal material degradation during the processing of biomedical thermoplastics. J Appl Polym Sci **120,** 2872, 2011.
11. Poh, P.S.P., Chhaya, M.P., Wunner, F.M., *et al.* Polylactides in additive biomanufacturing. Adv Drug Deliv Rev **107,** 228, 2016.
12. Choong, G.Y.H., and De Focatiis, D.S.A. A method for the determination and correction of the effect of thermal degradation on the viscoelastic properties of degradable polymers. Polym Degrad Stab **130,** 182, 2016.
13. Lehermeier, H.J., and Dorgan, J.R. Melt rheology of poly(lactic acid): consequences of blending chain architectures. Polym Eng Sci **41,** 2172, 2001.

14. Villalobos, M., Awojulu, A., Greeley, T., Turco, G., and Deeter, G. Oligomeric chain extenders for economic reprocessing and recycling of condensation plastics. Energy **31,** 3227, 2006.
15. Yang, L.X., Chen, X.S., and Jing, X.B. Stabilization of poly(lactic acid) by polycarbodiimide. Polym Degrad Stab **93,** 1923, 2008.
16. Tachibana, Y., Maeda, T., Ito, O., Maeda, Y., and Kunioka, M. Biobased myo-inositol as nucleator and stabilizer for poly(lactic acid). Polym Degrad Stab **95,** 1321, 2010.
17. Parthasarathy, L.K., Seelan, R.S., Tobias, C., Casanova, M.F., and Parthasarathy, R.N. Mammalian inositol 3-phosphate synthase: its role in the biosynthesis of brain inositol and its clinical use as a psychoactive agent. In: Majumder, A.L., Biswas, B.B., eds. Biology of Inositols and Phosphoinositides. Subcellular Biochemistry, vol 39. Boston, United States: Springer, pp. 293–314, 2006.
18. Ngo, T.D., Kashani, A., Imbalzano, G., Nguyen, K.T.Q., and Hui, D. Additive manufacturing (3D printing): a review of materials, methods, applications and challenges. Compos Part B Eng **143,** 172, 2018.
19. Norman E. Dowling. Mechanical Behavior of Materials. Boston, United States: Prentice Hall, 2013.
20. Harper, C.A. Modern Plastics Handbook. New York, United States: McGraw-Hill Professional, 2000.
21. Martin, O., and Avérous, L. Poly(lactic acid): plasticization and properties of biodegradable multiphase systems. Polymer **42**, 6209, 2001.
22. Ma, Z., Mao, Z., and Gao, C. Surface modification and property analysis of biomedical polymers used for tissue engineering. Colloids Surf B Biointerfaces **60,** 137, 2007.
23. Cámara-Torres, M., Sinha, R., Scopece, P., *et al.* Tuning cell behavior on 3D scaffolds fabricated by atmospheric plasma-assisted additive manufacturing. ACS Appl Mater Interfaces **13,** 3631-3644, 2021.
24. Zhu, Y., Leong, M.F., Ong, W.F., Chan-Park, M.B., and Chian, K.S. Esophageal epithelium regeneration on fibronectin grafted poly(l-lactide-co-caprolactone) (PLLC) nanofiber scaffold. Biomaterials **28,** 861, 2007.
25. Marchioli, G., Luca, A. Di, de Koning, E., *et al.* Hybrid polycaprolactone/alginate scaffolds functionalized with VEGF to promote de novo vessel formation for the transplantation of islets of langerhans. Adv Healthc Mater **5,** 1606, 2016.
26. Place, E.S., George, J.H., Williams, C.K., and Stevens, M.M. Synthetic polymer scaffolds for tissue engineering. Chem Soc Rev **38,** 1139, 2009.
27. Yoon, J.J., Kim, J.H., and Park, G. Dexamethasone-releasing biodegradable polymer scaffolds fabricated by a gas-foaming/salt-leaching method. Biomaterials **24,** 2323, 2003.
28. Bhutto, M.A., Wu, T., Sun, B., EI-Hamshary, H., Al-Deyab, S.S., and Mo, X. Fabrication and characterization of vitamin B5 loaded poly (l-lactide-co-caprolactone)/ silk fiber aligned electrospun nanofibers for schwann cell proliferation. Colloids Surf B Biointerfaces **144,** 108, 2016.
29. Damanik, F.F.R., van Blitterswijk, C., Rotmans, J., and Moroni, L. Enhancement of synthesis of extracellular matrix proteins on retinoic acid loaded electrospun scaffolds. J Mater Chem B **6,** 6468, 2018.
30. Yeong, W.Y., Chua, C.K., Leong, K.F., and Chandrasekaran, M. Rapid prototyping in tissue engineering: challenges and potential. Trends Biotechnol **22,** 643, 2004.
31. Anderson, P.H., and Atkins, G.J. The skeleton as an intracrine organ for vitamin D metabolism. Mol Aspects Med **29,** 397, 2008.
32. Hou, Y.-C., Lu, C.-L., Zheng, C.-M., *et al.* The role of vitamin D in modulating mesenchymal stem cells and endothelial progenitor cells for vascular calcification. Int J Mol Sci **21,** 2466, 2020.
33. Zhou, S., LeBoff, M.S., and Glowacki, J. Vitamin D metabolism and action in human bone marrow stromal cells. Endocrinology **151,** 14, 2010.
34. Geng, S., Zhou, S., Bi, Z., and Glowacki, J. Vitamin D metabolism in human bone marrow stromal (mesenchymal stem) cells. Metabolism **62,** 768, 2013.
35. Kang, D.J., Lee, H.S., Park, J.T., Bang, J.S., Hong, S.K., and Kim, T.Y. Optimization of culture conditions for the bioconversion of vitamin D3 to 1α,25-dihydroxyvitamin D3 using Pseudonocardia autotrophica ID9302. Biotechnol Bioprocess Eng **11,** 408, 2006.
36. Feldman, D., Pike, J.W., and Adams, J.S., eds. Vitamin D [Internet]. Elsevier, 2011. Available from: https://www.emerald.com/insight/content/doi/10.1108/nfs.2011.01741faa.017/full/html
37. Meng, F., Bertucci, C., Gao, Y., *et al.* Fibroblast growth factor 23 counters vitamin D metabolism and action in human mesenchymal stem cells. J Steroid Biochem Mol Biol **199,** 105587, 2020.
38. Sinha, R., Sanchez, A., Camara-Torres, M., *et al.* Additive manufactured scaffolds for bone tissue engineering: physical characterization of thermoplastic composites with functional fillers. ACS Appl Polym Mater **3,** 3788, 2021.
39. Macosko, C. Rheology: Principles, Measurements and Applications. New York, United States: Wiley-VCH, 1994.
40. Cámara-Torres, M., Sinha, R., Mota, C., and Moroni, L. Improving cell distribution on 3D additive manufactured scaffolds through engineered seeding media density and viscosity. Acta Biomater **101,** 183, 2020.
41. Gregory, C.A., Gunn, W.G., Peister, A., and Prockop, D.J. An Alizarin red-based assay of mineralization by adherent cells in culture: comparison with cetylpyridinium chloride extraction. Anal Biochem **329,** 77, 2004.
42. Morrison, F.A. Understanding Rheology, New York: Oxford University Press, 2001.
43. Kang, E.Y., Lih, E., Kim, I.H., Joung, Y.K., and Han, D.K. Effects of poly(L-lactide-ε-caprolactone) and magnesium hydroxide additives on physico-mechanical properties and degradation of poly(L-lactic acid). Biomater Res **20,** 7, 2016.
44. Speranza, V., De Meo, A., and Pantani, R. Thermal and hydrolytic degradation kinetics of PLA in the molten state. Polym Degrad Stab **100,** 37, 2014.
45. Rauwendaal, C. Polymer Extrusion [Internet]. München: Carl Hanser Verlag GmbH & Co. KG, 2014. Available from: http://www.hanser-elibrary.com/doi/book/10.3139/9781569905395
46. Meyers, M.A., and Chawla, K.K. Mechanical Behavior of Materials [Internet]. Cambridge: Cambridge University Press, 2008. Available from: http://ebooks.cambridge.org/ref/id/CBO9780511810947
47. Mallouk, R.S., and McKelvey, J.M. Power requirements of melt extruders. Ind Eng Chem **45,** 987, 1953.

48. Coppola, S., Grizzuti, N., and Maffettone, P.L. Microrheological modeling of flow-induced crystallization. Macromolecules **34,** 5030, 2001.
49. McIlroy, Claire, and Peter D. Olmsted. Deformation of an amorphous polymer during the fused-filament-fabrication method for additive manufacturing. J Rheol **61.2,** 379, 2017.
50. Pelc, B., and Marshall, D.H. Thermal transformation of cholecalciferol between 100–170°C. Steroids **31,** 23, 1978.
51. Jakobsen, J., and Knuthsen, P. Stability of vitamin D in foodstuffs during cooking. Food Chem **148,** 170, 2014.
52. Carley, J.F., and Strub, R.A. Application of theory to design of screw extruders. Ind Eng Chem **45,** 978, 1953.
53. Van Krevelen, D.W., and Te Nijenhuis, K. Properties of Polymers, 2009. Available from: https://www.elsevier.com/books/properties-of-polymers/van-krevelen/978-0-08-054819-7
54. Ward, I.M., and Sweeney, J. An Introduction to the Mechanical Properties of Solid Polymers, Hoboken, United States: John Wiley & Sons, 2004.
55. Utracki, L.A., and Wilkie, C.A., eds. Polymer Blends Handbook [Internet]. Dordrecht, Netherlands: Springer, 2014. Available from: http://link.springer.com/10.1007/978-94-007-6064-6
56. Tham, C.Y., Hamid, Z.A.A., Ahmad, Z.A., and Ismail, H. Surface engineered poly(lactic acid) (PLA) microspheres by chemical treatment for drug delivery system. Key Eng Mater **594–595,** 214, 2013.
57. Park, S., Yuan, Y., Choi, K., Choi, S.-O., and Kim, J. Doxorubicin release controlled by induced phase separation and use of a co-solvent. Materials (Basel) **11,** 681, 2018.
58. Almarri, F., Haq, N., Alanazi, F.K., *et al.* Solubility and thermodynamic function of vitamin D3 in different mono solvents. J Mol Liq **229,** 477, 2017.
59. Vlachopoulos, J., and Strutt, D. The role of rheology in polymer extrusion. Extrusion Minitec and Conference: From Basics to Recent Developments, Milan, Italy, November 2003, pp. 20–21.
60. Ignjatović, N., Uskoković, V., Ajduković, Z., and Uskoković, D. Multifunctional hydroxyapatite and poly(d,l-lactide-co-glycolide) nanoparticles for the local delivery of cholecalciferol. Mater Sci Eng C **33,** 943, 2013.
61. Fayyazbakhsh, F., Solati-Hashjin, M., Keshtkar, A., Shokrgozar, M.A., Dehghan, M.M., and Larijani, B. Release behavior and signaling effect of vitamin D3 in layered double hydroxides-hydroxyapatite/gelatin bone tissue engineering scaffold: an in vitro evaluation. Colloids Surf B Biointerfaces **158,** 697, 2017.
62. Fromigué, O., Marie, P.J., and Lomri, A. Differential effects of transforming growth factor β2, dexamethasone and 1,25-Dihydroxyvitamin D on human bone marrow stromal cells. Cytokine **9,** 613, 1997.
63. Lips, P. Vitamin D physiology. Prog Biophys Mol Biol **92,** 4, 2006.
64. Calore, A.R., Srinivas, V., Anand, S., *et al.* Shaping and properties of thermoplastic scaffolds in tissue regeneration: the effect of thermal history on polymer crystallization, surface characteristics and cell fate. J Mater Res **36,** 3914, 2021.
65. Deb, S., Reeves, A.A., and Lafortune, S. Simulation of physicochemical and pharmacokinetic properties of vitamin D3 and its natural derivatives. Pharmaceuticals **13,** 160, 2020.
66. Geng, S., Zhou, S., and Glowacki, J. Effects of 25-hydroxyvitamin D3 on proliferation and osteoblast differentiation of human marrow stromal cells require CYP27B1/1α-hydroxylase. J Bone Miner Res **26,** 1145, 2011.
67. Lian, J.B., and Stein, G.S. Concepts of osteoblast growth and differentiation: basis for modulation of bone cell development and tissue formation. Crit Rev Oral Biol Med **3,** 269, 1992.
68. Aubin, J.E. Regulation of osteoblast formation and function. Rev Endocr Metab Disord **2,** 81, 2001.
69. Freeman, F.E., Stevens, H.Y., Owens, P., Guldberg, R.E., and McNamara, L.M. Osteogenic differentiation of mesenchymal stem cells by mimicking the cellular niche of the endochondral template. Tissue Eng Part A **22,** 1176, 2016.
70. Costa, P.F., Puga, A.M., Díaz-Gomez, L., Concheiro, A., Busch, D.H., and Alvarez-Lorenzo, C. Additive manufacturing of scaffolds with dexamethasone controlled release for enhanced bone regeneration. Int J Pharm **496,** 541, 2015.
71. Wubneh, A., Tsekoura, E.K., Ayranci, C., and Uludağ, H. Current state of fabrication technologies and materials for bone tissue engineering. Acta Biomater **80,** 1, 2018.

Address correspondence to:
Lorenzo Moroni, Prof PhD
Complex Tissue Regeneration (CTR)
MERLN Institute for Technology-Inspired Regenerative Medicine
Maastricht University
Universiteitssingel 40
Maastricht 6229ER
The Netherlands

E-mail: l.moroni@maastrichtuniversity.nl

Received: February 28, 2022
Accepted: March 18, 2022
Online Publication Date: June 20, 2022